SPS/83-5 (ABM) January 1983

Characteristics of the radiation emitted by protons and antiprotons in an undulator

J. Bosser, L. Burnod, R. Coïsson*), G. Ferioli, J. Mann, F. Méot**)

Abstract

Spectral and angular distributions of visible radiation emitted by a high energy proton beam in an undulator have been measured for the first time. The same device has also allowed the direct visual observation of a beam of antiprotons. Interference in the radiation from two magnet edges and that between the edges and the undulator has also been seen in the angular distribution.

(submitted for publications to "Physics Letters")

---

*) present address: Istituto di Fisica, Università di Parma, 43100 Parma, Italy.

**) present address: CENG-LETI, B.P. 85X, F-38041, Genoble CEDEX, France.

Undulators, i.e. transverse periodic magnetic fields, in which electrons emit narrow-band synchrotron radiation (SR), or 'undulator radiation'(1), have been studied theoretically (2) and experimentally (3) and have been used to produce X-rays of high spectral brilliance. Even in modern high-energy machines, SR from protons has a critical frequency in the far infrared, however by using the 'edge effect' (4) it was possible to observe SR from protons produced by the SPS (400 GeV super proton synchrotron) in CERN (5) and to use this light as a transverse beam profile monitor (6). To increase the visible light intensity as well as to allow imaging of low current proton and antiproton beams at the storage energy (270 GeV, γ = 288), an undulator was installed (7), following an idea proposed a few years ago (8); the first measurements showed a power increase by a factor of 70.

In this letter we describe the measurements made at energies up to 400 GeV to check the characteristics of the light emitted by protons in an undulator, and the observation of interference effects in the light emitted from the two bending magnet edges, and from undulator and edges. We also report the first visual observation of an antiproton beam.

The radiation emitted by protons in a magnetic field, although not different in principle from that emitted by an electron (same spectrum for equivalent γ and equivalent trajectory), can be quite different in practical situations. This has been shown clearly in the properties of the 'edge effect' (5), which had not been observed before with electrons. This difference was also apparent in the present experiment as the narrow-band spectrum appeared at frequencies much higher than the critical one (either corresponding to the undulator peak field, or in the bending magnet).

For the theory, we refer to some review papers (9),(10),(11); we remind hereafter the main features verified by this experiment.

If the field B(z) (fig. 1) is the sum of an undulator (with peak field B_o, period $\lambda_o = 2\pi/k_o$ and length $L = n\lambda_o$) and edges of bending magnets M(z):

$$B(z) = -\sin k_o z \ \mathrm{rect}\ z/L + M(z - a + \Lambda/2) + M(-z - a - \Lambda/2) \quad (1)$$

the spectral brightness in a direction defined by the angles θ,ϕ can be written, for a current I at energy $\gamma\, mc^2$ ($\gamma^2 >> 1$) (11),(12):

$$\frac{dW}{d\Omega d\omega} = \frac{e^3 I}{8\pi^3 \varepsilon_o m^2 c} \gamma^2 F^2(\theta,\phi) \left|\tilde{B}(k)\right|^2 \quad (2)$$

with

$$k = \frac{1 + \gamma^2\theta^2}{2\gamma^2 c}\omega$$

F^2 describes the angular distribution of intensity:

$$F^2(\theta,\phi) = (1+\gamma^2\theta^2)^{-4}\left[(1-\gamma^2\theta^2+2\gamma^2\theta^2\sin^2\phi)^2 + 4\gamma^4\theta^4\sin^2\phi\cos^2\phi\right] \quad (3)$$

(the first term is the parallel component, the second is the perpendicular component).

and $\tilde{B}(k)$ is the Fourier transform of $B(z)$:

$$|\tilde{B}(k)|^2 = B_o^2\, n^2 \left(\frac{\sin(k-k_o)L/2}{(k-k_o)L/2}\right)^2 + 2|\tilde{M}(k)|^2 \sin^2 k\,\Lambda/2 + \qquad (4)$$

$$+ 4\,|\tilde{M}(k)|\,\frac{\sin(k-k_o)L/2}{(k-k_o)L/2}\,\sin k\,\Lambda/2\,\sin k\,a$$

The undulator term (the first) describes a narrow band of relative bandwidth $\Delta\omega/\omega \simeq 1/n$, around an angle-dependent central frequency:

$$\omega_1 = \frac{2\pi c}{\lambda_o}\,\frac{2\gamma^2}{1+\gamma^2\theta^2} = \frac{2\gamma^2 c\, k_o}{1+\gamma^2\theta^2} \qquad (5)$$

with total power

$$W = \frac{e^3\, I}{12\pi\varepsilon_o\, m^2c^2}\,\gamma^2\, B_o^2\, L \qquad (6)$$

The edge term $|\tilde{M}|^2 \sin^2 k\,\Lambda/2$ is as that calculated numerically in ref. 5, except that the edge separation is changed, which changes the period of the $\sin^2$ interference factor. With a filter at wavelength λ, the edge contribution has (ideally) zeroes for energies and angles satisfying the relation:

$$\frac{\Lambda}{2\gamma^2\lambda}\,(1+\gamma^2\theta^2) = \text{positive integer} \qquad (7)$$

and a cut-off at wavelengths $\sim d/2\gamma^2$ (see fig. 1).

The last term indicates interference between undulator and edges.

By integrating eq.2 over all angles to obtain $dW/d\omega$ the result is only a function of $(\omega/2\,\omega_o\gamma^2)$ where $\omega_o = k_o\,c$. This means that the same information on $dW/d\omega$ can be obtained by varying ω for a given γ or by fixing ω and plotting $dW/d\omega$ as a function of $1/\gamma$.

The parameters of our undulator are (7) : $n = 5$, $\lambda_o = 8.8$ cm, maximum peak field (vertical) $B \simeq 0.32$ T [deflection parameter $b = (e B_o \lambda_o / 2\pi\, m_o c) \simeq 10^{-3} \ll 1$]. The fixed magnet gap is 4.6 cm. The proton beam energy is up to 400 GeV in fixed target mode; it is 270 GeV in proton-antiproton storage ring operation with up to $5\cdot10^{11}$ protons (corresponding to $\sim$ 3 mA current) and $5\cdot10^{9}$ antiprotons stored. The other data given in fig. 1 are:
$\Lambda = 1070$ mm, $a = 55$ mm, $d \sim 5$ cm.

The experimental apparatus was remotely controlled (see fig. 2) and set up for beam image observation; therefore only minor modifications could be made for the present investigation such as placing narrow-band filters or lenses in front of the image detector. The order of magnitude of total power received by the detector was ~ 2 nW for a current of ~ 10 mA. The light power was verified to be proportional to the proton current and (see fig.3)

also proportional to the square of the undulator magnetic field. For a beam off-centre, it varied with the vertical displacement as B_o (y) (in our case $\partial^2 B_o/\partial y^2 = 16.4$ G mm^{-2}).

A typical result of power measurement made through a narrow-band filter with varying proton energy is reported in fig. 4. The reason for the difference between experimental data and expected results was accounted for by the limited angular acceptance, as was understood in the angular distribution measurements (see below) where the approximately square solid angle accepted was evident. For the same reason the degree of polarization was greater than 7/8 (7/8 would be the value for the whole radiation). The light was mainly polarized in the horizontal plane, which was the plane of the trajectory in the undulator. The energy γ_m corresponding to maximum power was in agreement with the integral of eq.2 over the angles; the maximum power corresponding to different filters (taking of course into account the different detector response) was proportional to $1/\lambda^2$, as for all filters $\Delta\lambda \simeq 50$ nm (then $\Delta\omega$ was proportional to $1/\lambda^2$).

A second set of measurements was made (again with filters, with $B_o \simeq 0.25$ T) by incorporating a lens of 150 mm focal distance in front of the detector, then imaging the back focal plane of the concave mirror onto the detector such that the intensity distribution on the second detector was proportional to the angular distribution of the emitted light. This data was recorded for various values of γ : a qualitative picture (photograph of TV display) is shown in fig. 6 for two values of λ . The angular opening for different values of λ and γ is described by eq.5 (see also fig. 5).

A plot of the intensity on a section ($\phi = \pm \pi/2$) of the angular distribution of the interference between edges (13), taking one line of the TV scan, is given in fig. 7.

Eventually, observation of angular distribution with various filters was repeated with the current in the undulator reversed. Fig. 8 is an example of how the interference between undulator and edges modifies the angular distribution: at angles where the amplitudes of light from the two sources are non-zero, there can be enhancement or suppression depending on the relative phase. Here the effect is small because the two sources have different angular distribution at the same λ, and interference occurs between an inner sidelobe of the undulator spectrum $\sin^2 [(k-k_o)L/2] / [(k-k_o)L/2]^2$ and an outer ring of the edges, therefore only a qualitative observation has been possible.

This set-up (fig. 2) will be used to monitor proton and antiproton beam profiles in the 270 GeV storage ring operation of the SPS. It has the property of being non-destructive and to allow continuous follow up of the evolution of the beam transverse distribution. It is possible to record individual circulating bunches with a resolution of the order of 0.2 mm (14).

REFERENCES

1. We use the expression 'synchrotron radiation' to indicate radiation from ultrarelativistic charged particles in any magnetic field; 'SR' is often used to indicate specifically the radiation in a uniform field (i.e. uniform over a distance $>R/\gamma$, where R is the radius of curvature).

2. V.L. Ginzburg, Izv.Akad.Nauk SSSR, Ser.Fiz 11, 165 (1947);
H. Motz, J.Appl.Phys.22, 527 (1951);
D.F. Alferov, Yu.A.Bashmakov and E.G. Bessonov, Zh.Tech.Fiz.43, 2126 (1973), Engl.Transl.:Sov.Phys.Tech.Phys.18, 1336 (1974).

3. see Proc.of Conf.on SR Instrum., Hamburg 1982, to be published in Nucl. Instrum.& Meth.: papers by G. Brown et al., H. Kitamura et al., and M.M. Nikitin and A.F. Medvedov; see also C. Bazin et al., J.de Phys. Lett.41, L-547 (1980).

4. R. Coïsson, Optics Comm.,22, 135 (1977).

5. R. Bossart, J. Bosser, L. Burnod, R. Coïsson, E. D'Amico, A. Hofmann, and J. Mann, Nucl.Instr.& Meth.,164, 375 (1979).

6. R. Bossart, J. Bosser, L. Burnod, E. D'Amico, G. Ferioli, J. Mann and F. Méot, Nucl.Instr.& Meth.,184, 349 (1981).

7. J. Bosser, L. Burnod, F. Méot, A. Riche, SPS/ABM/JB/Report 80-8.

   F. Méot, Thesis, CERN-SPS 81-21 (ABM) (1981).

8. R. Coïsson, Nucl.Instr.& Meth.,143, 241 (1977); R. Coïsson, IEEE Trans. NS-24, 1681 (1977);
D.F. Alferov and E.G. Bessonov, Pisma v Zh.Tekh.Fiz.,3, 828 (1977).

9. D.F. Alferov, Yu.A.Bashmakov and E.G. Bessonov, 'Undulator Radiation', Lebedev Phys.Inst.Ser.80,ed.N.G. Basov; Engl.Transl.N.Y.Consultants Bureau 1976.

10. A. Hofmann, Phys.Rep. 5, 253-281 (1980).

11. R. Coïsson, Phys.Rev. A20, 524 (1979).

12. We therefore neglect the deflection in bending magnets and the results tend to ∞ as $\omega \to 0$, but give good results in the visible ($\omega >> \omega_c$) (4),(5),(11).

13. Interference effects in SR, related to the present one, have been observed also with electrons: M.M. Nikitin, A.F. Medvedev, M.B. Moisseyev and V.Ya.Epp, ZhEksp.i Teor,Fiz.79, 163 (1980);
D.F. Alferov and Yu.A.Bashmakov, Pis'ma JETF 34, 15 (1981);
V.I. Alekseyev, E.G. Bessonov, A.V. Kalinin and V.A. Krasikov, FIAN 228, Moskow 1981.

14. The monitor is described in a paper submitted to IEEE Trans.N.S.

FIGURE CAPTIONS

Fig. 1 Magnetic field of the whole structure (undulator plus edges of bending magnets) as a function of co-ordinate z along proton trajectory a is the distance between centre of undulator and mid-point between edges.

Fig. 2 Experimental apparatus: the light emitted in the undulator U by protons (right) and by antiprotons (left) is deflected by surface mirrors M outside a quartz window and towards concave mirrors C which form an image of the undulator on the image detectors (silicon intensified targets (6)). Narrow-band filters or lenses can be placed in front of the detector. A 3x3 mm square image on the detectors (collected in 40 ms) is memorized in digital form.

Fig. 3 Light power from undulator at fixed energy (270 GeV) and proton current, vs square of undulator field B .

Fig. 4 Power through a narrow-band filter (λ = 0.55 μm, $\Delta\lambda$ = 50 nm) as a function of γ. The continuous line indicates the ideal power collected over all angles, the circles are the experimental data collected over a limited solid angle (a square $\sim 1/\gamma$ times $1/\gamma$).

Fig. 5 Aperture of the radiation cone as a function of energy, for various wavelengths.

Fig. 6 Photographs of TV displays of angular distribution of light for two wavelengths, for several values of γ , within the limits of angular acceptance. At low energy only the undulator appears, then the spot becomes a ring of increasing radius; at higher energies, rings due to interference between edges appear and move outwards.

Fig. 7 Angular intensity distribution ($\phi = \pm \pi/2$) of light through a λ = 0.7 μm filter. This shows the evolution of the rings due to interference of edges: the position of the minima as a function of γ is described by eq.7 (taking into account filter bandwidth).

Fig. 8 Angular distribution (γ = 405): a) without undulator (edges only), b) with undulator, c) with undulator with reversed current (then magnetic field changed in sign). The change in intermediate rings is due to interference of undulator radiation and 'edge effect'.

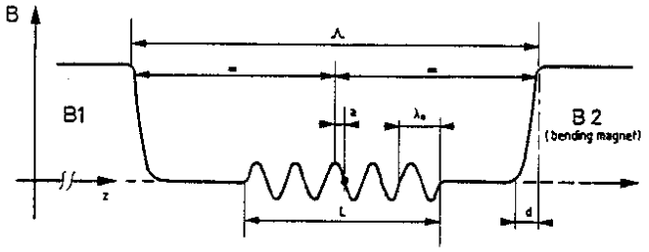

Fig. 1

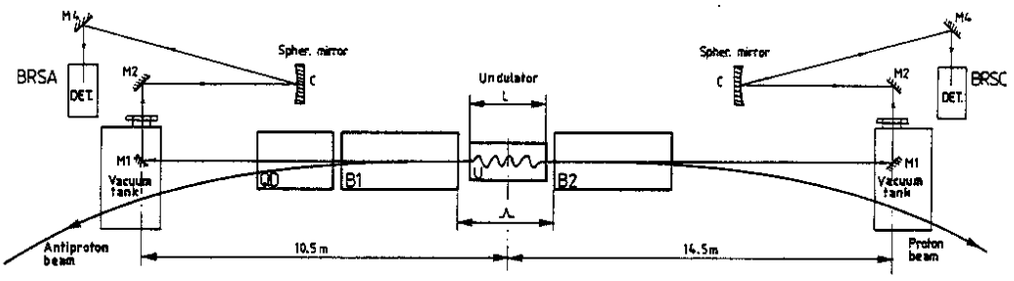

Fig. 2

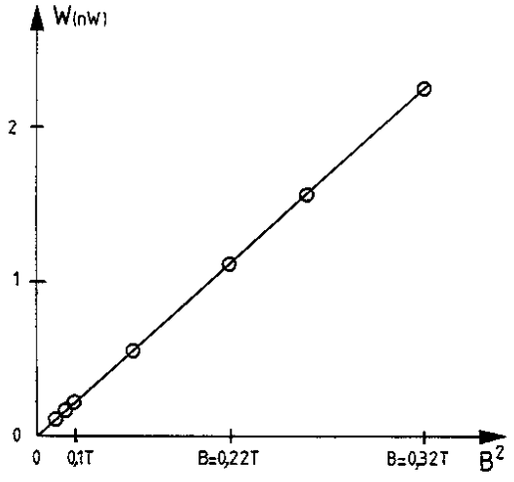

Fig. 3

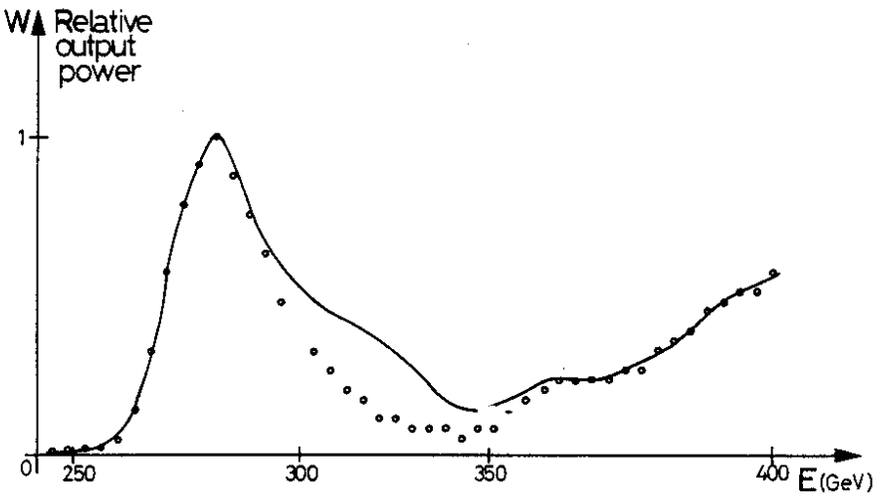

Fig. 4

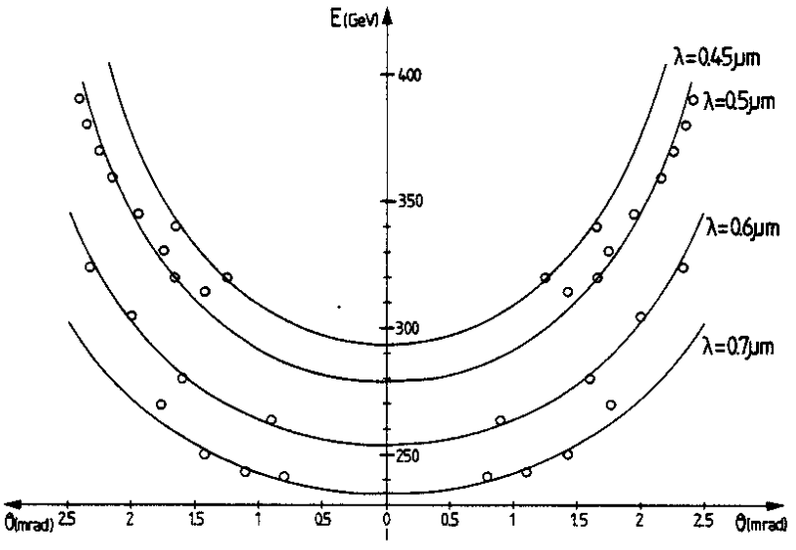

Fig. 5

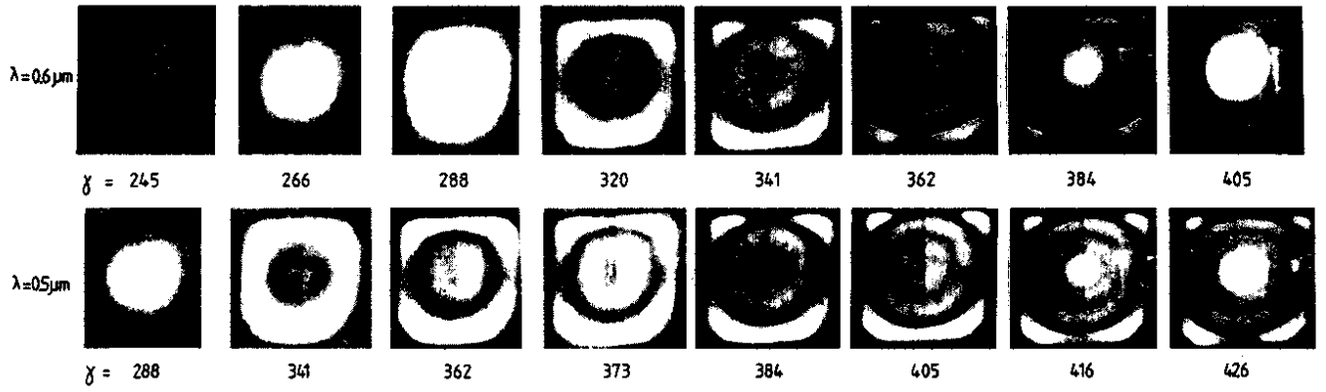

Fig. 6

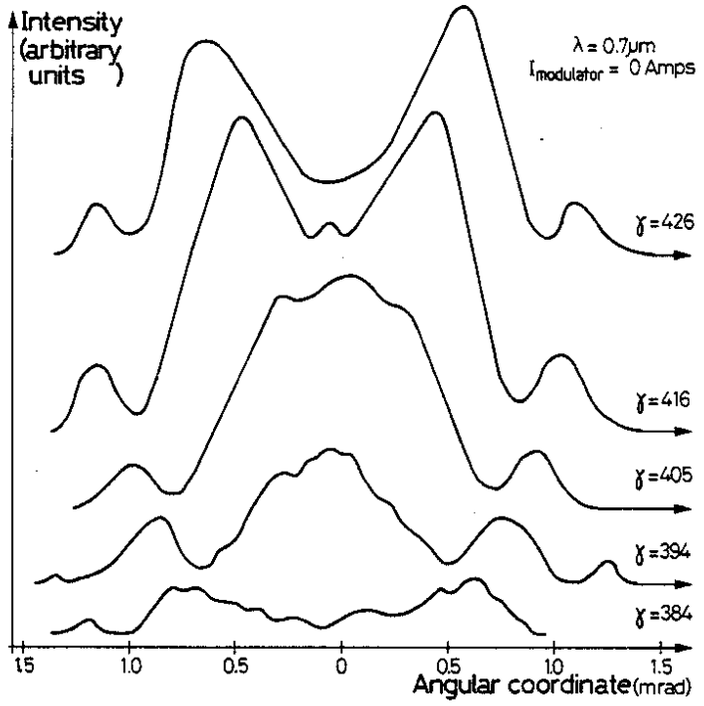
Intensity
(arbitrary
units)
λ = 0.7μm
I modulator = 0 Amps
γ=426
γ=416
γ=405
γ=394
γ=384
1.5
1.0
0.5
0
0.5
1.0
1.5
Angular coordinate (mrad)

Fig. 7

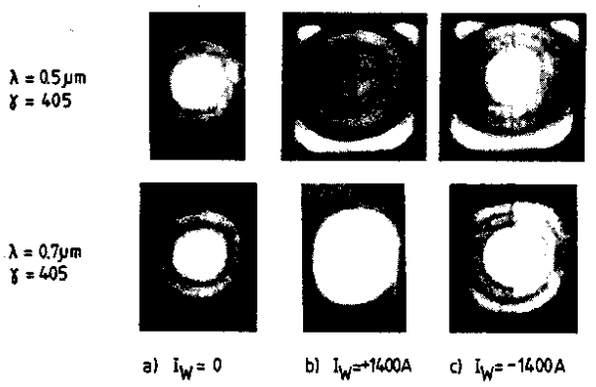
λ = 0.5μm
γ = 405
λ = 0.7μm
γ = 405
a) $I_W = 0$
b) $I_W = +1400A$
c) $I_W = -1400A$

Fig. 8